Supplementary Information (SI) for Soft Matter.

Particle-Wall Alignment Interaction and Active Brownian Diffusion Through Narrow Channels

Poulami Bag, Shubhadip Nayak, and Pulak K. Ghosh†

Department of Chemistry, Presidency University, Kolkata 700073, India

† Email: pulak.chem@presiuniv.ac.in

Supporting information

SI-1: Chirality in active particle

Chirality is a property of being chiral. An object having a distinguishable mirror image is known as a chiral one. In the context of the present work, certain non-spherical active colloidal or natural microswimmers are chiral in nature. Artificial chiral active particles can be created due to fabrication defects or by purposeful designs. Chiral active particles have intrinsic torque, leading to a spinning motion as a result of translation-rotation coupling in the hydrodynamic sense (Kraft et al., [1]) or an asymmetry in the propulsion mechanism [2]. In contrast, achiral active particles do not have intrinsic spinning motion due to structural and functional symmetry. Therefore, the transport and diffusion characteristics of chiral particles are expected to be notably different from achiral ones. Additionally, the dynamical properties of a chiral active particle heavily depend on the direction and magnitude of the torques. Particles with positive and negative torques are known as levogyre and dextrogyre, respectively.

Several previous works focus on the design and synthesis of chiral particles aiming at specific applications [3-5]. For example, Ghosh et al. [3] reported the design and function of chiral active particles that can be operated in water with high (micron-level) precision using homogeneous magnetic fields. Schamel et al., [4] use chiral colloids to demonstrate the Baranova and Zel'dovich propeller effect.

SI-2: Relevance of parameters used in simulation

Considering time in second (s) and length in micrometer (μm) the units of the simulation parameter are: self-propulsion speed v_0μm/s, rotational diffusion D_θ s^{-1}, Translational diffusion

$D_0 \mu m^2/s, \omega_0\ s^{-1}$, $\Omega\ s^{-1}$, and λ μm and $\chi\ \mu m^{-1}$. The exact values of the self-propulsion parameters can be found in the experimental works[17, review]..

Let's first consider rotational diffusion time. Its value can be approximately estimated using Einstein–Smoluchowski relation,

$$D_\theta = \frac{k_B T}{8\pi\eta R^3}.$$

In a study by Volpe et al. [17], it was found that the experimental value of the rotational diffusion time of an active Janus particle closely matches the estimation based on the Einstein–Smoluchowski relation. Further, they reported that for a Janus particle (silica sphere with gold cap) of size 2.13 μm, rotational relaxation time is about 200 second in mixture of water and 2,6-lutidine. However,the rotational diffusion time scale can be adjusted by modifying the particle size and the viscosity of the medium.

The self-propulsion speed v_0: Reference [17] presents v_0 as a function of light intensities and demonstrates that v_0 varies between 0.05 μm/s and 0.4 μm/s. Other sources (refer to table 1 in ref[28]) indicate that the self-propulsion speed greatly depends on the type of active particles, the size of the active surface, and the self-propulsion mechanism involved. The self-propulsion velocity can range from 0.05 μm/s to upwards of 100mm/s. Consequently, the self-propulsion parameters, D_θ and v_0, used in our simulation can be accessed through in experiments.

The amplitude of the chiral torque (Ω) depends on particle shape and anisotropy in the propulsion mechanism [1-2]. In our analysis, we consider the situation when $\Omega > \{\omega_0, D_\theta\}$ as well as the other possibilities $\Omega \approx \{\omega_0, D_\theta\}$ and $\Omega < \{\omega_0, D_\theta\}$.

Particle-wall alignment interaction induced torque ω_0: Our model of alignment interaction rests on the fact that near the walls, particle-wall interaction stabilizes the active particles at some specific orientations. This assertion is in accord with previous studies [6-9]. For example, based on extensive study on a catalytically active Janus particle W. E. Uspal et al. [6] demonstrate that in the close vicinity of hard planar walls, active Janus particles display a steady direction and height above the wall. Properties of such hovering states largely depend on the catalyst coverage and the interactions of the product molecules with the different parts of the particle. Recently [7],

using holographic imaging it was demonstrated that in swimming bacteria, like E. coli, the mechanism of wall entrapment is an intricate interplay of hydrodynamic and steric interactions with a strongly anisotropic character. It has been observed that in the trapped state, swimming bacteria move with the average body axis pointing into the walls [7]. The amplitude of orientation-dependent alignment interaction and torque largely depends on the dielectric properties of the material used to prepare active particles, fuel distribution near the walls, and hydrodynamic interaction near the wall. Thus, ω_0 can be treated as an independent model parameter. ω_0 can be larger than D_θ or vice-versa. To understand, the possible impact of alignment interactions in all regimes, we numerically estimated the diffusion coefficient as a function of ω_0/D_θ, as well as, ω_0/Ω.

SI-3: Rotational relaxation and Mean square displacement of a chiral active particle in free space

A. Auto-correlations function of self-propulsion velocity components

As the x and y directional self-propulsion motions of an active particle in the free space are statistically independent,

$$\langle \cos\theta(t)\sin\theta(0)\rangle = \langle \sin\theta(t)\cos\theta(0)\rangle = 0.$$

Also, the average behaviors of self-propulsion motion in both the x and y directions are the same. Thus, we can write,

$$\langle \cos\theta(t)\cos\theta(0)\rangle = \langle \sin\theta(t)\sin\theta(0)\rangle. \quad \text{- - - - (S1)}$$

:

This auto-correlation function can be re-arranged as,

$$\langle \cos\theta(t)\cos\theta(0)\rangle = \frac{1}{2}\mathrm{Re}\left\{\left\langle e^{-i[\theta(t)-\theta(0)]}\right\rangle\right\} \quad \text{- - - - (S2)}$$

Where, Re{…} represents the real part of the complex quantity. As the stochastic variable $\Delta\theta(t) = \theta(t) - \theta(0)$ follows Gaussian statistics, and in the absence of particle-wall alignment interaction, its first two moments are given by,

$$\langle \Delta\theta\rangle = \Omega t \quad \text{and} \quad \langle \Delta\theta^2\rangle - \langle \Delta\theta\rangle^2 = 2D_\theta t \quad \text{- - - - (S3)}$$

Cumulant expansion of the stochastic Gaussian variable Δθ(t) produces,

$$\left\langle \exp\left[-i\Delta\theta(t)\right]\right\rangle = \exp\left[i\left\langle \Delta\theta(t)\right\rangle - \frac{\left\langle \Delta\theta^2\right\rangle - \left\langle \Delta\theta\right\rangle^2}{2}\right] = \exp\left[i\Omega t - D_\theta t\right]$$

Using this expression in (S2), we obtain Eq.(7) of main text,

$$\left\langle \cos\theta(t)\cos\theta(0)\right\rangle = \frac{1}{2}\cos(\Omega t)\, e^{-D_\theta |t|} \quad - \; - \; - \; -(S4)$$

B. **Mean square displacement**

Integration of the stochastic differential Eq. (2) of main text produces,

$$\Delta x(t) = x(t) - x(0) = \mathrm{v}_0 \int_0^t \cos\theta(t')dt' + \sqrt{2D_0}\int_0^t \xi_x(t')dt'.$$

Corresponding square displacement is given by,

$$\Delta x^2(t) = [x(t)-x(0)]^2 = \mathrm{v}_0^2 \int_0^t dt'' \int_0^t \cos\theta(t'')\cos\theta(t')dt' + 2\mathrm{v}_0\sqrt{2D_0}\int_0^t dt'' \int_0^t \cos\theta(t'')\xi_x(t')dt'$$

$$+ 2D_0 \int_0^t dt'' \int_0^t \xi_x(t'')\xi_x(t')dt'.$$

Now, taking average over noise realizations,

$$\left\langle \Delta x^2(t)\right\rangle = \mathrm{v}_0^2 \int_0^t dt'' \int_0^t \left\langle \cos\theta(t'')\cos\theta(t')\right\rangle dt' + 2D_0 \int_0^t dt'' \int_0^t \left\langle \xi_x(t'')\xi_x(t')\right\rangle dt'.$$

Making using of Eq.(5) and (7) of main text, we obtain

$$\left\langle \Delta x^2(t)\right\rangle = \frac{\mathrm{v}_0^2}{2}\int_0^t dt'' \int_0^t \cos\Omega(t'-t'')\exp\left[-\mathrm{D}_\theta \,|\, t'-t''\,|\right]dt' + 2D_0 \int_0^t dt'' \int_0^t \delta(t'-t'')\, dt'\,.$$

Straightforward integration of the above equation produces Eq.(9) of main text

$$\left\langle \Delta x^2(t)\right\rangle = \mathrm{v}_0^2\left[\frac{D_\theta t}{D_\theta^2+\Omega^2} + \frac{D_\theta^2-\Omega^2}{\left(D_\theta^2+\Omega^2\right)^2}\left(\cos\Omega t\, e^{-D_\theta t} - 1\right)\right] - \frac{2\mathrm{v}_0^2 D_\theta \Omega}{\left(D_\theta^2+\Omega^2\right)^2}\sin\Omega t\, e^{-D_\theta t} + 2\mathrm{D}_0 t$$

SI-4: Numerical simulation method

The final terms of all three equations (2-4) in the main text [$\xi_x(t)$, $\xi_y(t)$, $\xi_\theta(t)$] represent zero mean white noise with Gaussian distribution. The times evolution equations for the stochastic variables x, y and θ can be expressed as a general form of stochastic differential equation:

$$\dot{X} = A(X) + B\xi(t)$$

Where, X ={x, y and θ} and the first term on the right hand side of the above equation is the deterministic and second one that is stochastic. There are several numerical schemes (Heun's method [11], stochastic runge-kutta methods [12,13], Milstein algorithm [14]) to solve this equation. All scheme produces the same results when the numerical integration time steps are small enough. In these schemes, Gaussian white noises [$\xi_x(t)$, $\xi_y(t)$, $\xi_\theta(t)$] are generated from two random numbers which are uniformly distributed on the unit interval. Box–Mueller algorithm is used to convert them into a normal distribution with unit variance and zero mean.

Boundary conditions:Our simulations consider confining walls to be perfectly reflecting. The wall-particle collisions have been modeled by the elastic reflection of instantaneous velocity at the boundary [15, 16] . The reflecting wall exerts a force, $(\dot{\boldsymbol{r}}.\hat{n})\hat{n}/\mu$ if the particle is at the wall and zero otherwise. Where, $\hat{n}$ is the local normal to the wall pointing outwards and μ represents the mobility. As a result of the interaction with the hard wall, the particle's instantaneous velocity direction gets reverted at the boundaries.

SI-5: Derivation of Eq(12)

For configuration I, the active particles tend to stick against the top (bottom) wall [see panel (a) in Fig.S1] at an angle $\pi/2$ ($-\pi/2$) when ω_0 is stronger than D_θ. For this orientation of $\mathbf{v}_0$, the displacement due to self-propulsion motion along the channel axis is zero. However, self-propulsion contributes in diffusion when $\mathbf{v_0}$ direction gets tilted due to rotational diffusion [see panel (b) in Fig.S1]

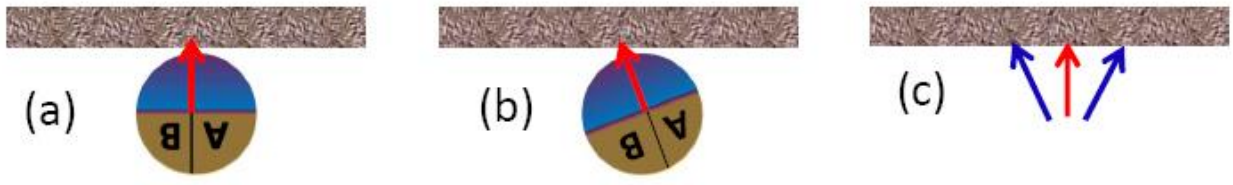

Figure S1: This figure schematically illustrates: (a) the stable orientation of the active particle against the top wall at $\theta = \pi/2$, (b) a small deviation of the orientation from the stable angle, (c) two slanted blue arrows represent two orientational states (kinematic states) at $\theta = \pi/2 - \sigma$ and $\theta = \pi/2 + \sigma$ around the stable orientation (red arrow).

Probability of tilting $\mathbf{v_0}$ by an angle $\delta\theta$ about the stable orientation,

$$p(\delta\theta) = N \exp\left[-\frac{\Delta V(\delta\theta)}{k_B T} \right] \quad - - - - \text{(S4)}$$

Where N is a normalization constant. For $\delta\theta$ orientation fluctuations about the stable $\mathbf{v_0}$ direction at the top wall, the change in interaction potential is given by,

$$\Delta V(\delta\theta) = V\left(\frac{\pi}{2} + \delta\theta\right) - V\left(\frac{\pi}{2}\right)$$

If $\delta\theta$ is small,

$$V\left(\frac{\pi}{2} + \delta\theta\right) = V\left(\frac{\pi}{2}\right) + V'\left(\frac{\pi}{2}\right)\delta\theta + \frac{1}{2!}V''\left(\frac{\pi}{2}\right)\delta\theta^2 + ... \approx V\left(\frac{\pi}{2}\right) + \frac{1}{2!}V''\left(\frac{\pi}{2}\right)\delta\theta^2$$

Thus,

$$\Delta V(\delta\theta) \approx V''\left(\frac{\pi}{2}\right)\delta\theta^2$$

Now considering particle-wall interaction (equation 1 in the main text) in proper dimension,

$$\Delta V(\delta\theta) \approx \frac{1}{2}\gamma_R V_t''\left(\frac{\pi}{2}\right)\delta\theta^2 = \frac{1}{2}\tilde{\omega}_0 \delta\theta^2 = \frac{1}{2}\gamma_R \omega_0 \delta\theta^2 \quad - - - - \text{(S5)}$$

Combining Eq.(S4) and Eq.(S5), we get

$$p(\delta\theta) = N\exp\left[-\frac{\gamma_R \omega_0 \delta\theta^2}{k_B T}\right] = N\exp\left[-\frac{\omega_0}{2D_\theta}\delta\theta^2\right] \text{ - - - - (S6)}$$

Where, $D_\theta = k_B T/\gamma_R$. On normalization of the above distribution function, we obtain

$$p(\delta\theta) = \sqrt{\frac{\omega_0}{2\pi D_\theta}}\exp\left[-\frac{\omega_0}{2D_\theta}\delta\theta^2\right] \text{ - - - - (S7)}$$

The variance σ^2 of this distribution is given by,

$$\sigma^2 = \frac{\omega_0}{D_\theta} \text{ - - - - (S8)}$$

To estimate $\mathbf{v_0}$ orientation fluctuation-induced diffusion, we assume that on an average, self-propulsion velocity direction switches between two kinematic states , $\theta = \pi/2-\sigma$ and $\pi/2+\sigma$ (as shown in Fig.S1(c)) over an approximate time period $1/\omega_0$. For these two $\mathbf{v_0}$ orientations, the components of self-propulsion along the channel axis are,

$$\pm v_0 \sin\left(\sqrt{\frac{\omega_0}{D_\theta}}\right)$$

Considering the switching of v_0 direction between these two kinematic states as a dichotomic process, we obtain Eq.(11) of the main text .

SI-6: Symmetry axis of the JP and the self propulsion velocity direction

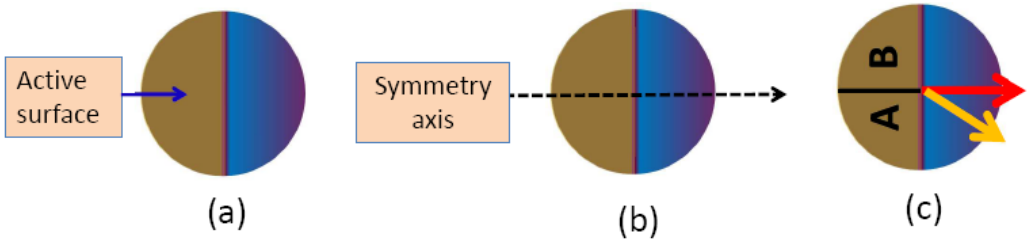

Figure S2: (a) Schematics of Janus particle depicting: (a) active surface, (b) symmetry axis bisecting active surface (indicated by dashed line), and (c) possible direction of self-propulsion

velocity with respect to the symmetry axis. Note that for a perfectly symmetric JP, the symmetry axis we refer to is C_∞ and the symmetry point group of the particle is $C_{\infty v}$.

In Figure S2, we schematically illustrate the direction of self-propulsion velocity ($\mathbf{v_0}$) with respect to the symmetry axis of the JP. Here, The symmetry axis (or plane in the case of 3D) refers to a line (or plane) that bisects the coated hemisphere (active hemisphere). The two equal parts of the bisected active hemisphere are indicated by A and B [see Fig.S2(c)]. The average direction of $\mathbf{v_0}$ aligns with the symmetry axis, but the instantaneous direction fluctuates around it (see Figure 1(g, h, i) in reference [17]). Let's consider the instantaneous rates of self-phoresis in parts A and B of the active surface as r_A and r_B, respectively. Only when $r_A = r_B$, the direction of $\mathbf{v_0}$ is expected to be coincide with the symmetric axis. On the other hand, if r_A does not equal r_B, the direction of $\mathbf{v_0}$ does not fall on the symmetric axis. In Figure S2(c), the yellow arrow indicates the direction of $\mathbf{v_0}$ when r_A is less than r_B. In the context of particle-wall alignment interaction, near the walls, for some orientation of the particle, part A and part B of the active surface are not equally exposed to the fuel. Thus, $r_A \neq r_B$ and $\mathbf{v_0}$ does not fall on the symmetric axis.

References

[1] Kraft, D. J., R. Wittkowski, B. ten Hagen, K. V. Edmond, D. J. Pine, and H. Löwen, 2013, "Brownian motion and the hydrodynamic friction matrix for colloidal particles of complex shape," Phys. Rev. E 88, 050301.

[2] Kümmel, F., B. ten Hagen, R. Wittkowski, I. Buttinoni, R. Eichhorn, G. Volpe, H. Löwen, and C. Bechinger, 2013, "Circular motion of asymmetric self-propelling particles," Phys. Rev. Lett. 110, 198302.

[3] A. Ghosh and P. Fischer, Nano Letters, 2009, 9, 2243–2245.

[4]D. Schamel, M. Pfeifer, J. G. Gibbs, B. Miksch, A. G. Mark and P. Fischer, Journal of the American Chemical Society, 2013, 135, 12353–12359.

[5] J. T. Collins, C. Kuppe, D. C. Hooper, C. Sibilia, M. Centini and V. K. Valev, Advanced Optical Materials, 2017, 5, 1700182.

[6] W. E. Uspal, M. N. Popescu, S. Dietrich and M. Tasinkevych, Soft Matter, 2015, 11, 434–438.

[7] S. Bianchi, F. Saglimbeni and R. Di Leonardo, Phys. Rev. X, 2017, 7, 011010.

[8] A. Mozaffari, N. Sharifi-Mood, J. Koplik and C. Maldarelli, Phys. Rev. Fluids, 2018, 3, 014104.

[9] A. Poddar, A. Bandopadhyay and S. Chakraborty, Journal of Fluid Mechanics, 2020, 894, A11

[10] P. Czajka, J. M. Antosiewicz and M. D. A.Cugosz, ACS Omega, 2019, 4, 17016–17030

[11] Süli, Endre; Mayers, David , An Introduction to Numerical Analysis, Cambridge University Press, (2003), ISBN 0-521-00794-1.

[12] A. Tocino and R.Ardanuy, Runge–Kutta methods for numerical solution of stochastic differential equations, Journal of Computational and Applied Mathematics, Volume 138, Issue 2, 15 January 2002, Pages 219-241

[13] Andreas Rößler, Runge–Kutta Methods for the Strong Approximation of Solutions of Stochastic Differential Equations, SIAM Journal on Numerical AnalysisVol. 48, Iss. 3 (2010)10.1137/09076636X

[14] P. Kloeden and E. Platen, Numerical Solutions of Stochastic Differential Equations (Springer, Berlin, 1999).

[15] Y. Fily, A. Baskaran and M. F. Hagan, Soft Matter, 2014, 10, 5609–5617

[16] P. K. Ghosh, V. R. Misko, F. Marchesoni and F. Nori, Phys. Rev. Lett., 2013, 110, 268301.

[17] G. Volpe, I. Buttinoni, D. Vogt, H.-J. Kümmerer and C. Bechinger, Soft Matter, 2011, 7, 8810.

[18] C. Bechinger, R. Di Leonardo, H. Löwen, C. Reichhardt, G. Volpe and G. Volpe, Rev. Mod. Phys., 2016, 88, 045006.